CRISPR/Cas9 KOs of p53 and STAT1 in HEK293 Cells

Melanie Terveer

S4109309

Research Project Biomedical Sciences (WBBY902-10)

BSM5 Aging Research ERIBA

Supervisor: Mathilde Broekhuis

Foijer Lab – Genomic Instability in Development and Disease

University of Groningen

07-06-2022

Abstract

Chromosomal instability (CIN) is a process characterized by chromosome mis-segregation often occurring in cancer. As a result of CIN, a downstream inflammatory response is activated, which leads to cancer cell clearance. STAT1 and p53 are genes which are known to be involved in this inflammatory response, while OAS1 and IFIT1 are theorized to be involved. To better understand the role of these genes, the plan was to make knockouts using the CRISPR/Cas9 mechanism. HEK293 cells were transfected with plasmids containing sgRNAs for p53 and STAT1. Validation of the knockouts was performed, using PCR and subsequent sequencing and western blot. The western blot showed that there was no decrease in STAT1 protein levels in the STAT1 KO sample. Conversely, there was a slight reduction of p53 protein levels in the p53 KO sample, but PCR and Sanger sequencing showed that there was no mutation at the p53 sgRNA target site of p53 KO cells. Therefore, it seems that the knockout of p53 and STAT1 in HEK293 cells was unsuccessful.

Introduction

Cells with chromosomal instability (CIN) experience segregation deficiencies during mitosis, which results in cells displaying structural and/or chromosomal abnormalities, like aneuploidy. Aneuploidy does not only cause growth defects, but it can also increase cell growth and survival [Ben-David et al., 2014]. This is supported by the fact that approximately 2 out of 3 human tumors are aneuploid [Duijf et al., 2013]. The consequence of CIN and ensued aneuploidy is a reduced fitness of the cell, which can trigger reduced proliferation potential, apoptosis, and/or senescence [Schukken & Foijer, 2017]. An important player in the mechanism that prevents early chromosome mis-segregation is the mitotic spindle assembly checkpoint (SAC) [A. Musacchio & E.D. Salmon, 2007]. Defects in SAC can cause CIN and consequently aneuploidy [Chen et al., 2022]. SAC monitors whether all kinetochores have properly attached to the mitotic spindle, and if not, it inhibits further progression of mitosis [A. Musacchio, 2015].

In untransformed cells, p53 recognizes aberration and damage in DNA, such as aneuploidy. p53 is a well-known tumour-suppressor gene. Activation of p53 leads to cell cycle arrest, DNA repair, or even apoptosis [Kadioglu et al., 2021]. It has been shown that a loss of p53 and CIN are associated with tumorigenesis [Foijer, et al., 2017; Foijer, et al., 2014]. Mutations in p53 substantially reduce the number of cells that arrest in the G1 phase due to chromosome mis-segregation. However, aneuploidy itself does not necessarily lead to p53 activation and G1 arrest, but the stress caused by chromosome mis-segregation does lead to p53 activation [Santaguida et al., 2017]. Furthermore, it was found that mutations in p53 enable both euploid and aneuploid tumour cell growth. Thus, while loss of p53 is common in CIN tumours, it is not necessarily a hallmark for CIN. However, specifically, aneuploid cancers inactivate STAT1 signalling to evade an immune response [Schubert et al., 2021].

As a result of CIN, DNA from the nucleus may leak into the cytosol. This can happen either directly or through the formation and successive rupture of extranuclear DNA-containing structures, called micronuclei [Hatch et al., 2013]. The presence of cytosolic DNA triggers DNA sensors, such as cyclic GMP-AMP synthase (cGAS), which subsequently activate the type I interferon response, which induces the production of pro-inflammatory cytokines, immune activation, and ultimately leads to clearance of the cancer cell, see figure 1 [Hatch et al., 2013; Mackenzie et al., 2017].

NF-κB can be activated in two ways; canonical and non-canonical. When activated, the canonical NF-κB can induce a variety of cytokines and chemokines, which are known for their role in tumour progression and clearance [Hellweg, 2015]. Interestingly, non-canonical NF-κB signalling has been demonstrated to promote cancer metastasis [Bakhoum et al., 2018; Hou et al., 2018]. CIN triggers IL6/STAT3-mediated signalling, which is dependent on both cGAS/STING as well as the non-canonical NF-κB pathway, see figure 1 [Hong et al., 2022]. It was found that both interferon and NF-κB signalling are involved in the protection of cells against CIN-induced cell death. STING modulates both cell death-promoting STAT1 and cell survival-promoting STAT3 [Hong et al., 2022; Chen et al., 2022].

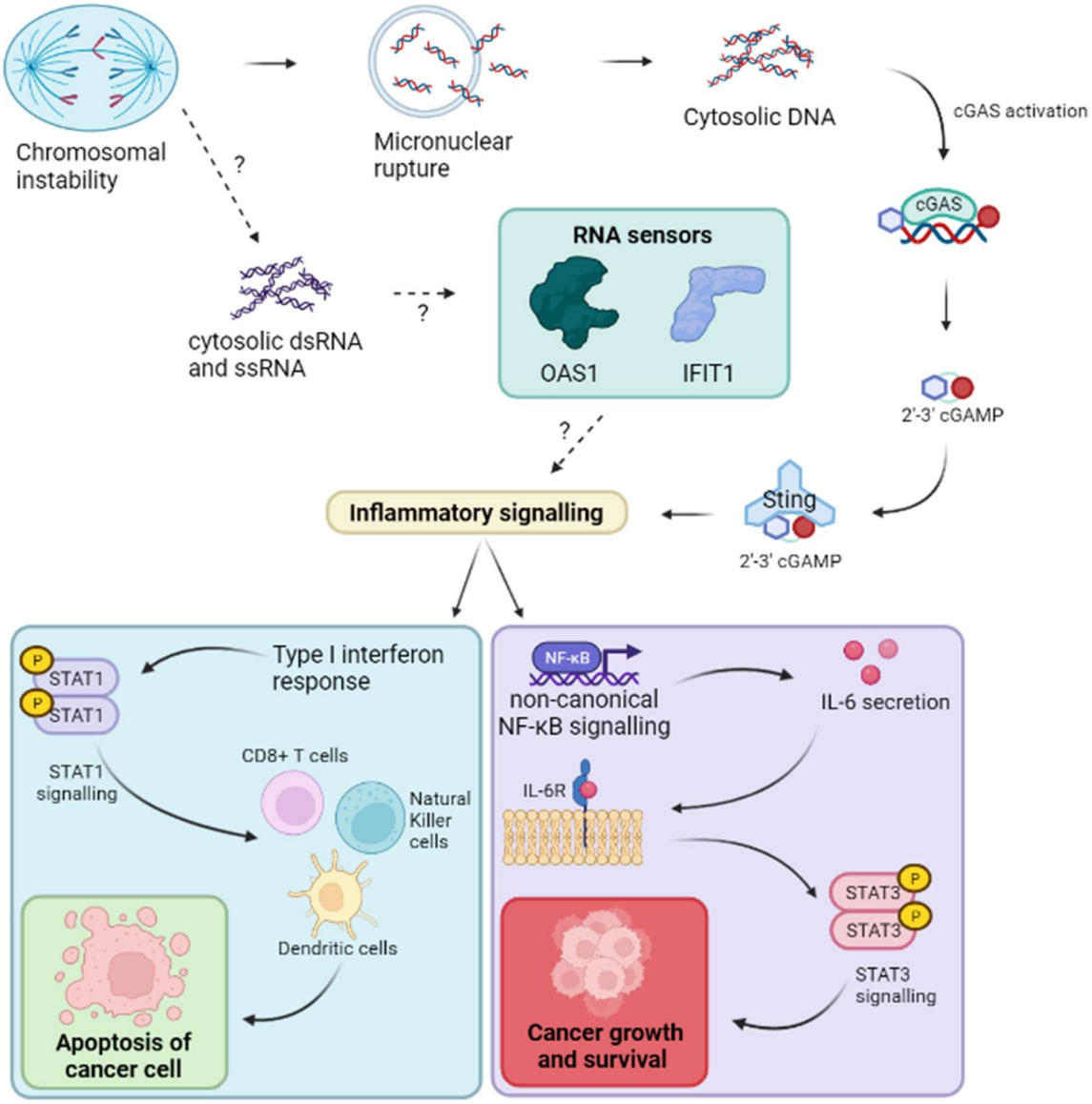

Figure 1: Schematic overview of inflammatory response induced by CIN [adapted from Hong et al., 2022 and created in BioRender.com]
cGAS gets activated by cytosolic DNA, which leads to the synthesis of cGAMP [Hong et al., 2022]. cGAMP, in turn, activates STING which subsequently activates the type I interferon response or the non-canonical NF-κB pathway. When activated, the type I interferon response results in the recruitment of immune cells, such as dendritic cells, CD8+ T cells and Natural Killer cells, and the subsequent clearance of the CIN cancer cell [Chen et al., 2022]. Activation of the non-canonical NF-κB pathway induces the secretion of IL-6, which binds to the IL-6 receptor (IL-6R) advancing to the activation of STAT3 signalling which leads to cell survival and growth [Hong et al., 2022]. RNA sensors, like OAS1 and IFIT1, might also get activated by cytosolic RNA as a result of CIN, which can possibly lead to inflammatory signalling as described in this figure.

The larger aim of the project is to better understand how the inflammatory response induced by chromosomal instability contributes to the survival of cells with CIN and how aneuploid cancers manage to avoid the immune cells that were activated after this response. In our project, we will start with the first steps. These involve making knock-out cell lines for two important control genes involved in the regulation of the response to CIN; STAT1 and p53, and knock-outs of two cytokine-encoding genes, OAS1 and IFIT1.

The role of STAT1 and p53 genes in the response against CIN is already known. For that reason, they will be inactivated and used as controls. Based on bioinformatic analysis, OAS1 and IFIT1 are thought to be involved in this inflammatory pathway. Interferon-induced protein with tetratricopeptide repeats 1 (IFIT1) is a detector for cell-intrinsic viral RNA and is implicated to have a role in cancer progression and metastasis [Pinto et al., 2015; Pidugu, et al., 2019]. 2'-5'-oligoadenylate synthase 1 (OAS1) is a cellular double-strand RNA sensor, which functions as part of the innate immune response against viruses [Di, et al., 2020]. However, the exact role of these genes in the inflammatory response induced by CIN is still unknown. Hence, we want to experimentally determine whether these genes are indeed involved in this inflammatory response. Therefore, we will target HEK293 cells with sgRNAs targeting p53, STAT1, OAS1, and IFIT1, we will assess whether the sgRNAs work by using quantitative RT PCR and western blot we will determine whether our strategy indeed leads to knockout HEK293 cells.

HEK293 cells will be used because they are robust, adherent cells with high reproducibility and are relatively easy to maintain. Additionally, they are efficient at protein production and amenable to transfection and CRISPR/Cas9 genome-editing [Thomas & Smart, 2005]. Furthermore, CIN can be induced in these HEK293 cells, so KO cells without CIN can be compared to KO cells with CIN.

To create knock-outs (KOs) we will be using the CRISPR/Cas9 system. CRISPR/Cas9 is a two-component gene-editing mechanism that enables genetic modification by single-guide RNA (sgRNA) [Shojaei Baghini et al., 2021]. The two components of this system are the nuclease Cas9 and sgRNA. The sgRNA recruits the Cas9 protein to the target site where it will induce a double-strand DNA break [Sun et al., 2016]. The CRISPR/Cas9 system has two main double-strand break repair mechanisms; non-homologous end-joining (NHEJ) and homology-directed repair (HDR) [Wan et al., 2021]. For this project, we will rely on NHEJ, via which the double-strand breaks will be repaired. However, this is an error-prone mechanism, frequently resulting in insertions/deletions (INDELs) [Ishibashi et al., 2020]. In exons, INDELs can create a frameshift mutation, which can induce nonsense-mediated decay and thus an inactivated gene [Tuladhar et al., 2019].

To start off, sgRNAs will be designed and cloned into pX-459 V2.0 (Cas9-2A-Puro) vectors. Furthermore, it will be assessed whether sgRNAs were incorporated into the plasmid using Sanger sequencing. HEK293 cells will be transfected with these plasmids. Lastly, PCR and western blot will be used to validate whether the knockouts were successful. The western blot showed no reduction in STAT1 protein levels, while there was a minor reduction in p53 protein levels. PCR and Sanger sequencing of the p53 gene showed that there were no mutations at the p53 sgRNA target site of p53 KO cells. In conclusion, the knockout of p53 and STAT1 in HEK293 cells seems unsuccessful.

Material and Methods

Guide RNA and primer design for OAS1 & IFIT1

Guide RNAs targeting the human OAS1 and IFIT1 gene were designed by in silico cloning using CRISPR design in Benchling. Guide RNAs were chosen based on their inclusion of all isoforms of the OAS1 and IFIT1 protein. For the BbsI restriction site oligos were designed with a 5'-CACC (forward) and 5'-AAAC (reverse) overhang. The following guide RNAs were chosen for OAS1: gRNA1 targeting exon 1 (5'-CTTGGACACACACACAGGGT-3'), gRNA2 targeting exon 1 (5'-TGGCATGGTTGATTTGCATG-3') and gRNA3 targeting exon 2 (5'-GTACGAAGCTGAGCGCACGG-3').

The following guide RNAs were chosen for IFIT1: gRNA1 targeting exon 2 (5'-TCGAAAGACATAGGTCTGTG-3') and gRNA2 targeting exon 2 (5'-GTGTCCAGAAATAGACTGTG-3'). Primers were designed surrounding the sgRNA regions to later validate the knockout in HEK293 cells. Guide RNAs and primers were ordered from the IDT company. Guide RNAs for p53 and STAT1 were readily available and contained the following sequences: 5'-GAAGGGACAGAAGATGACAG-3' and 5'-GTCCGCAACTATAGTGAACCT-3', respectively.

Cloning of sgRNAs in vector & growing *E. coli* containing the vector

Cloning was performed as described in Nature Protocols [Ran et al., 2013], in short: (1) phosphorylation and annealing of the oligos, (2) the digestion-ligation reaction, (3) treatment of the ligation reaction with PlasmidSafe exonuclease and (4) transformation in bacteria. The backbone vector used is pX459 V2.0 (WT-2A-Puro V2.0 62988 from Addgene). The bacteria used were *Escherichia coli* (*E. coli*) strain DH5α. The bacteria were transformed with the vector using the heat-shock method at 42 °C. The transformed bacteria were plated on LB + agar plates with ampicillin (Amp) (100 ng/µL) and incubated overnight at 37 °C. Ampicillin resistance is encoded in the vector so that bacteria containing the vector are selected.

Multiple colonies (6 for both STAT1 and p53; 4 for both OAS1 and IFIT1 per sgRNA) were selected and grown in 3 mL LB medium with ampicillin (100 ng/µL) for 24 hours at 37 °C in the shaking incubator. glycerol stocks of all clones were prepared and stored in -80 °C freezer. Thermo Scientific™ GeneJET Plasmid Miniprep Kit was used to isolate the plasmid DNA of the remaining cell cultures; the purification protocol for high-copy number plasmids was applied. DNA concentrations were measured by NanoDrop and plasmids were sent to Eurofins for Sanger sequencing with primer (U6 fwd: 5'-GAGGGCCTATTTCCCATGATTCC-3'), to check which clones had inserted the correct sgRNA. DNA sequences were analysed and aligned with plasmid pX459 V2.0+sgRNA.

The following steps were only performed for sgRNAs of p53 and STAT1. One clone was chosen per sgRNA based on the alignment. A starter culture was created from the glycerol stock. The starter culture was 1000x diluted in 100 mL LB + Amp and incubated in the shaking incubator at 37 °C for 24 hours. NucleoBond Xtra Midi kit for transfection-grade plasmid DNA was used to isolate plasmids from the p53 and STAT1 sgRNA cultures. The pellet containing the purified plasmids was resuspended with 250 µL TE buffer and stored at 4 °C. DNA concentration was measured using NanoDrop.

Cell culture
Human embryonic kidney (HEK293) cells were thawed and seeded in a 25cm2 culture flask and cultured in 5 mL Dulbecco's modified Eagle medium (DMEM) supplemented with 10% Fetal Bovine Serum (FBS) and 100U/mL Penicillin-Streptomycin. The HEK293 cells were grown in a 37 °C incubator for two days. For cell passage, first, the medium was discarded. Next, the cells were washed with Phosphate Buffered Saline (PBS) and subsequently discarded. After 0.25% trypsin was added to the adherent cells, the cells were incubated for 5 min at 37°C. After incubation, 5 mL DMEM medium was added to the cells, and vigorously pipetted and diluted into three 75 cm2 culture flasks. For optimal growth, the cells got fresh medium after 4 days.

Transfection
One day before transfection, cells were plated on 6-well plates. For this, the medium was discarded, and the cells were washed with 10 mL PBS and treated with 3 mL 0.25% trypsin. After incubation of 5 min at 37 °C, 4 mL medium was added to each flask, cells were collected and centrifuged for 5 mins at 300x g at 22 °C, after which the medium was discarded and a cell pellet remained. The pellet was resuspended in 5 mL fresh DMEM. 15 µL medium containing the cells was put in a 1 mL Eppendorf tube, to which 15 µL Trypan Blue was added. With an automatic cell counter, the cells were counted. 1 mL contained 6.5 x 106 cells. Approximately 300,000 cells were plated on each well of a 6-well plate in 2 mL medium. The plates were incubated in a 37 °C incubator for a day.

The FuGENE® HD Transfection Reagent protocol was prepared by mixing 9 µL FuGENE® reagent and 3 µg of each plasmid DNA (ratio FuGENE:DNA = 3 µL:1 µg), Opti-MEM was added to reach a total volume of 200 µL. The reaction was incubated for 15 minutes at room temperature and after which it was distributed to the 6-well plates. The plasmids used for transfection contained sgRNAs targeting p53 or STAT1 and three controls. The positive control was the empty pX459-puro-Cas9 plasmid, without sgRNA. The pX458-GFP (green fluorescent protein) plasmid was used to visualize transfection efficiency. The negative control was cells containing no plasmids, which is a control for puromycin resistance.

Puromycin selection
Puromycin selection was started 72 hours after transfection. HEK293 cells that were transfected on 6-well plates, were treated with 2 mL DMEM medium with puromycin (2 µg/mL) (p53, STAT1, pX459 and negative control) or 2 mL DMEM medium (pX458). The plates were incubated at 37 °C. After 24 hours, the medium was refreshed.

Validation of the STAT1 and p53 knockout using PCR and western blot
The cells not used for puromycin selection were used for the validation of KO of STAT1 and p53. Cells were harvested by vigorously washing with PBS and split in half for DNA and protein extraction. The tubes were centrifuged for 5 minutes at 300x g at 22 °C. The PBS was discarded and the tubes were stored at -20 °C. For the PCR of the p53 gene, the cell pellet containing the STAT1, p53, pX459 plasmids and the negative control, were used. The DNA was isolated from the cells using the DNeasy® Blood & Tissue Kit and eluted in 100 µL AE buffer. To determine the DNA concentration, the NanoDrop was used. The samples were diluted to 50 ng/µL. 50 µL PCR mix containing p53 forward and p53 reverse primer (0.5 µM) and 100 ng plasmid DNA (50 ng/µL) was prepared for each sample. Either, p53, STAT1, pX459 or the negative control isolated DNA. Water was used as a negative control for PCR. PCR bands at 740 bp (p53) for the samples p53 and STAT1 were cut out of the agarose gel. DNA was isolated from the agarose gel with the Zymo DNA clean and concentrator kit and sent to IDT company for sequencing.

For the western blot, the general protocol for western blotting from BioRad was used. The cell pellets (p53, STAT1, pX458, pX459 and negative control) were resuspended in 100 µL ELB buffer, to which 1/50 diluted protease inhibitor was added. The cells were centrifuged in a tabletop centrifuge at 4 °C for 5 min at 500 x g, after which the cell debris was discarded. The western blot samples were mixed 5:1 with sample buffer (SDS + DTT), after which they were heated for 5 minutes at 96 °C. Subsequently, samples were run on an SDS-Page gel on a running buffer for one hour at 100 V followed by an hour at 200 V.

The proteins were transferred onto polyvinylidene difluoride (PVDF) membranes followed by 5-minute incubation at room temperature with a blocking buffer. The PVDF membranes were incubated overnight with anti-p53 (SC-126, mouse host, diluted 1:500 in blocking buffer), anti-Actin 4970 (rabbit host, 1:5000 in blocking buffer), anti-STAT1 (9772S, rabbit host, 1:1000 in blocking buffer) and anti-Actin 3700 (mouse host, 1:5000 in blocking buffer) at 4 °C on a roller. The membranes were washed three times with TBS-Tween (TBS-T) and incubated with secondary antibodies, anti-rabbit-IR800 (αR, 1:10000 in blocking buffer) and anti-mouse-IR700 (αM, 1:10000), for one hour at room temperature with gentle agitation followed by three washes with TBS-T and one final one with TBS. In the western blot, the colour tags for αR and αM were green and red, respectively. The blots were imaged and quantified with the Odyssey system.

Results

Validation of sgRNA incorporation in plasmids

To create knockouts, sgRNAs for p53, STAT1, IFIT1, and OAS1 were cloned into backbone vectors. The resulting sequences were compared to plasmid templates to validate whether the sgRNAs were indeed taken up by the plasmids. In Benchling the plasmid sequences were aligned to the corresponding complementing templates (see figure 1A, for example). For each sgRNA design, there was a plasmid clone that had correctly incorporated the sgRNAs, because the DNA sequence of the template and the cloned vectors were identical at the sgRNA site (figure 1B-H). Therefore we can conclude that for all 4 genes plasmid cloning was successful.

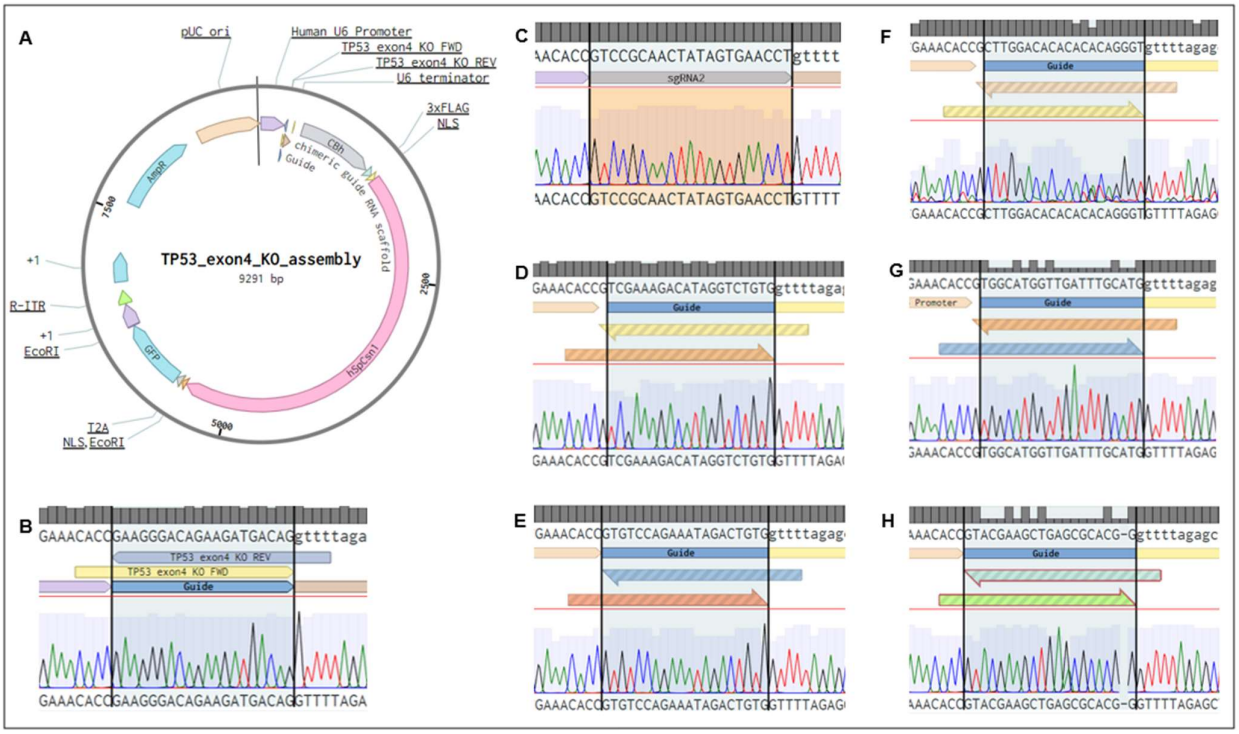

Figure 2: Benchling alignment validation for sgRNA in plasmids

A. Vector map of pX459_V2.0_p53

B-H. Sequence alignment of sgRNA in exon 4 of p53 (B), exon 10 of STAT1 (C), exon 2 of IFIT1 #1 (D), exon 2 of IFIT 1 #2 (E), exon 1 of OAS1 #1 (F), exon 1 of OAS1 #2 (G), and exon 2 of OAS1 (H). The DNA sequence on top is the template sequence and the bottom DNA sequence is the sequence of the plasmid with the incorporated sgRNA. Alignments created in Benchling.

HEK293 cells were chosen as target cells
To create knockout cell lines, we used HEK293 cells. HEK293 cells are derived from the primary cultures of Human Embryonic Kidney cells by transformation with sheared fragments of adenovirus 5 DNA [Shaw et al., 2002]. HEK293 cells are often used in research using CRISPR/Cas9 for knocking out genes [Ebina et al., 2013; Chen et al., 2013; Cheng et al., 2013]. According to cytogenetic analysis, the 293 cell line is pseudo-triploid [Bylund et al., 2004]. The average chromosome number in HEK293 cells is 64, in 30% of the cells, with higher ploidy occurring in 4.2% of the cells. They have three copies of the X chromosome, and a 4 kbp fragment of AD5 incorporated into chromosome 19, which display cytogenetic instability [Synthego, n.d.].

Transfection of HEK293 cells with pX458-GFP, pX459-Puro-p53 and pX459-Puro-STAT1
HEK293 cells were transfected with pX459 vectors containing sgRNAs for STAT1 or p53. Positive control cells were transfected with pX458-GFP vectors. Negative control cells were transfected with the empty pX459 vector. A second negative control consisted of cells transfected with saline (no vector). Positive control cells were visualized by microscopy (see figure 3A-F). The majority of these cells were positive for GFP expression, as visible in an overlay of bright-field and fluorescence microscopy (figure 3C and 3F). As most of the positive control cells seemed to be successfully transfected, no puromycin selection was done before knockout validation (western blot and PCR) of HEK293 cells transfected with vectors containing sgRNAs.

Puromycin selection was performed on the remaining part of the HEK293 cells transfected with pX459 vectors. Cells were incubated in DMEM with puromycin (2 µg/mL) for 24 hours at 37 °C, between 72 and 96 hours after transfection. Microscopy showed that cells transfected with pX459 vectors were still adherent (figure 3G). Negative control cells without the pX459 vector had a round morphology and were largely detached from the culture flask (figure 3H). The cells were incubated in puromycin containing DMEM for more than 24 hours (after microscopy). At later time points, cells with the pX459 vector also detached from the culture flask and had a round morphology, indicating that they died.

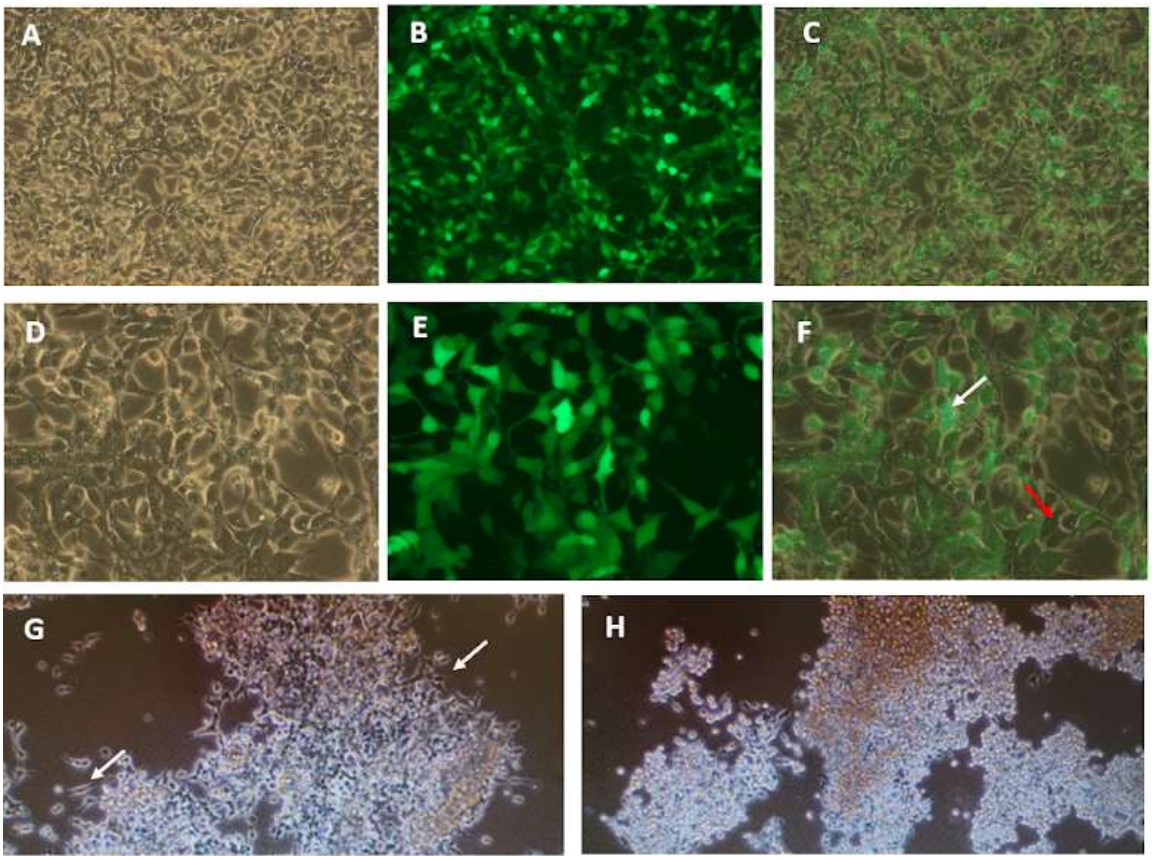

Figure 3: Transfection of HEK293 cells

A. Bright-field microscope picture of HEK293 cells 24 hours after transfection with the vector pX458, containing green-fluorescent protein (GFP). 40x magnification.
B. The same picture as (A) was visualized using fluorescent light, which visualizes GFP as green fluorescence.
C. Overlay of panel (A) and (B), showing positive and negative cells for the GFP vector.
D. Fluorescence microscopy picture of HEK293 cells that were transfected with the pX458-GFP vector. 100x magnification.
E. The same picture as (D) using fluorescent light. GFP is visible as green fluorescence.
F. Overlay of panel (D) and (E), showing the cells that are positive and negative for the GFP vector. Examples of positive and negative cells are given by white and red arrows, respectively.
G. Microscopic image of HEK293 cells transfected with empty backbone vector pX459 V2.0 (WT-2A-Puro) after 24 hours of incubation in DMEM with puromycin (2 µg/mL). Cell cultures of HEK293 cells transfected with pX459, containing sgRNAs for STAT1 or p53, looked similar (not shown), 24 hours after incubation in DMEM with puromycin (2 µg/mL) at 37 °C. Puromycin selection was started 72 hours after transfection. Cell attachment is visible, indicated with white arrows.
H. Microscopic image of HEK293 cells treated with saline transfection reagent (negative control) after 24 hours of incubation in DMEM with puromycin (2 µg/mL) at 37°C. The vast majority of cells had detached from the culture flask and had a round morphology.

Validation of STAT1 and p53 KO HEK293 cells

p53 and STAT1 KO HEK293 cells were generated with the CRISPR/Cas9 technology. sgRNAs for p53 and STAT1 were cloned into pX459 V2.0 vectors, which were transfected into the HEK293 cells. The sgRNA-Cas9 complex would cause a double-stranded break. Non-Homologous End-Joining (NHEJ) would lead to insertions or deletions in exon 4 for p53 and in exon 10 for STAT1, theoretically leading to a frameshift 2 out of 3 times. PCR and sequencing were used to validate the mutation in the p53 gene. HEK293 samples, containing the p53 plasmid and 4 controls were separated on fragment size, using p53 primers (see figure 4A). This figure shows that each sample, except water, contained the p53 fragment, but between 100 and 500 bp non-specific binding occurred in all samples, except the water lane.

The p53 PCR band was cut out of the agarose gel for cells transfected with sgRNAs for p53 or STAT1 (negative control). The p53 gene was isolated from these samples with Zymo DNA clean and concentrator kit and sent for Sanger sequencing. Alignment of the sgRNA sequence with a wildtype (wt) p53 template, showed that there were no mutations in the sgRNA sequence of the STAT1 sample, as expected (see figure 4B). There were also no mutations in the sgRNA sequence of the p53 sample (figure 4B), thereby indicating that the KOs were probably not successful. Interestingly, the sequence preceding the sgRNA contained a lot of mismatches in both the cells transfected with sgRNAs for p53 and the negative control. This indicates that the HEK293 cells probably already had mutations in the p53 gene.

Furthermore, KOs of STAT1 and p53 HEK293 cells were validated by western blot. The absence or decrease in protein levels of p53 and STAT1 indicates a KO (figure 4C-D). Protein level was quantified with the ratio of intensity STAT1/Actin and p53/Actin (figure 4C-F). The Actin 3700 band was used for both the p53 and STAT1 quantification, as the Actin 4970 was not visible. The western blot showed that there was no decrease in STAT1 protein expression (figure 4E), which suggests that there were probably no STAT1 KOs HEK293 cells. However, the p53 protein level was slightly decreased in cells targeted for p53 KO (figure 4F). Remarkably, a non-specific band was detected at around 100 kDa in all lanes (figure 4C and 4D). In addition, there was a green band visible at approximately 50 kDa in figure 4D.

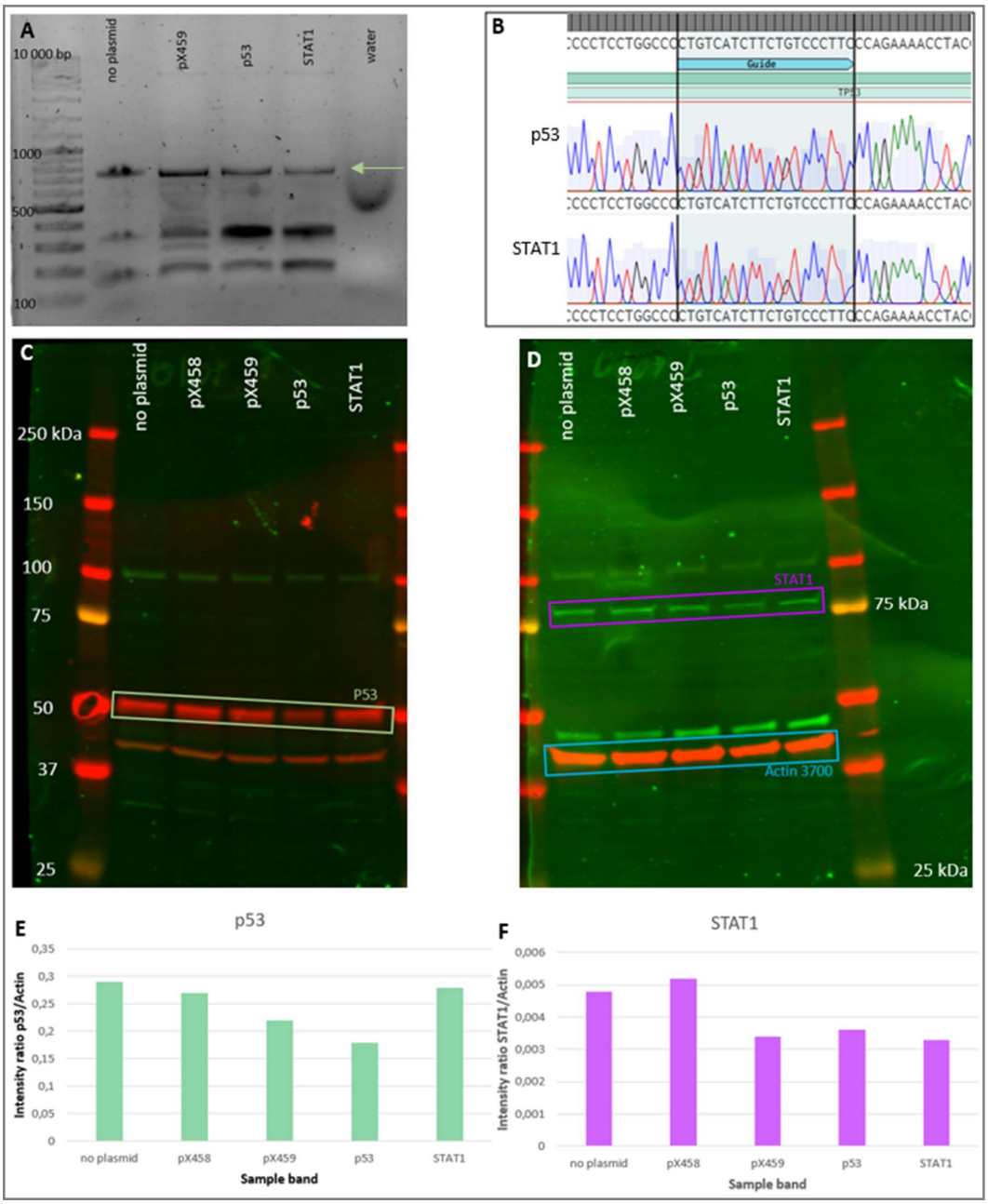

Figure 4: PCR and western blot in transfected HEK293 cells

A. PCR of the p53 gene in HEK293 cells, 72 hours after transfection with pX459 with sgRNA for p53. The presence of the p53 gene was validated for the cells targeted for p53 KO and control cells, as seen in the bands at 740 bp (green arrow). The negative control ("water") did not contain a DNA sample and correspondingly showed no p53 band.
B. Sanger sequencing results of p53 editing in STAT1 and p53 targeted cells, compared to the wt p53 gene template.
C. Western blot analysis of p53 expression in HEK293 genome-edited cell lines with, from right to left, no DNA control, pX458-GFP plasmid, pX459 plasmid, KO p53 and KO STAT1.
D. Western blot analysis of STAT1 expression in HEK293 genome-edited cell lines.
E. Quantification of the p53 protein levels measured in the western blot (C). Expression levels of p53 were compared to actin expression levels.
F. Quantification of the STAT1 protein levels measured in the western blot (D). Expression levels of STAT1 were compared to actin expression levels.

Discussion

The objective of this study was to generate knockout cell lines for p53, STAT1, IFIT1 and OAS1 using CRISPR/Cas9 in HEK293 cells. These findings are important in the context of the inflammatory response induced by chromosomal instability, in which p53 and STAT1 are known to be involved, and in which IFIT1 and OAS1 are theorized to be involved. Research with IFIT1 and OAS1 KO cell lines may illuminate this biological pathway that is mediated by CIN. Previously it was found that loss of p53 and CIN collaborate in tumorigenesis in various models [Foijer et al., 2014]. In addition, the inactivation of STAT1 is a conserved process for CIN tolerance in many cell types and species [Schubert et al., 2021]. In order to create a knockout, sgRNAs were designed and cloned into plasmids, which were transfected into HEK293 cells. Due to time restrictions, transfection was only done in plasmids containing sgRNAs for STAT1 and p53. Further validation steps with western blot and PCR indicated that no p53 or STAT1 knockout cell lines were realized.

For the transfection method, a transient transfection agent called FuGENE was used. Thus, the transfected cells take up the plasmids, but the plasmid is not integrated into their genome [Marucci et al., 2011]. Therefore, some cells will have the knockout, however, the daughter cells may lose the vector, thereby losing puromycin resistance. As the western blot and PCR were performed with cells that grew for over 72 hours, it is possible that the plasmids with puromycin resistance had already been diluted. The transient transfection method can be inefficient, therefore transduction with lentiviral vectors can be a prefered method as this leads to the incorporation of the vector in the genome thereby preventing dilution [Mao et al., 2015]. However, a disadvantage of lentiviral vectors is that the whole vector, including the Cas9 protein, is permanently integrated into the host cell, which can lead to possible insertional mutagenesis [Vannucci et al., 2013].

Moreover, we performed the puromycin selection well after 72 hours of transfection, therefore it is reasonable to assume that there had already been dilution of the plasmid in the cell culture. All transfected cell cultures (empty pX459, pX459-p53, pX459-STAT1, and negative control) detached and died between the 24-96 hours after puromycin selection. The presumed reason for this, was because the puromycin selection was maintained for too long leading to the death of HEK293 cells, even though the transfection was successful. Furthermore, the cells were not cultured in optimal conditions, as the cell density was too high leading to medium exhaustion.

The western blot for STAT1 did not show a decrease in protein expression level of the STAT1 band (figure 4 D/F). Conversely, it did seem that there was less protein expression in the p53 sample of this blot, but this was most likely due to an overall lower protein load as the actin was also decreased in this well. Furthermore, this blot showed a clear band around 50 kDa. The band for STAT1 is around 80 kDa, but it appears that the STAT1 antibody used, 9172S, also binds around 50 kDa [Cellsignal Signaling Technology, n.d.]. In addition, there were green bands for all samples around 100 kDa, in both the STAT1 and p53 blot, this is most probably due to non-specific binding caused by incomplete blocking.

The quantification of the western blot for p53 showed a slight decrease in protein expression of the p53 samples compared to the controls. However, this data must be interpreted with caution, because the p53 sample of the p53 blot was compared to Actin 3700 on the STAT1 blot (see figure 4 C/D). The reason for this discrepancy, was because the secondary antibody failed, resulting in no actin bands in the p53 blot to compare it with. As there was less signal in the p53 sample of the STAT1 blot, it is reasonable to assume that there was also less signal in the p53 sample of the p53 blot. Indicating that there could be less protein loaded in the p53 sample in general and thus the minor decrease could be coincidental. This is a likely scenario, as the PCR and subsequent sequencing results (figure 4 A/B) show that we did not generate a p53 KO cell line.

The Sanger sequencing of the isolated PCR fragments of p53 KO showed no mutations at the sgRNA site. However, many base-pairs did not align with the wildtype (wt) p53 template preceding the sgRNA sequence. This phenomenon was present in both the control and the supposedly p53 KO cells. It could be possible that the HEK293 cells used had a mutated p53 gene of their own, however, the HEK293 cell line usually carries a wt p53 gene [Sun et al., 2010]. This led to the speculation that these mutations could have impaired the primer binding, possibly leading to the impairment of the Sanger sequencing.

Although the sgRNA was incorporated correctly into the pX459 V2.0 vector, the efficiency of the sgRNA and Cas9 protein is unknown. Thus, it is uncertain whether the Cas9 protein is guided to the targeted location and whether gene inactivation is achieved. The reason is that the CRISPR/Cas9 knockout system is based on NHEJ after a double-strand DNA break, leading to a frameshift 2 out of 3 times [Wan et al., 2021]. Thus, not all alleles will have the inactivated gene. As full knockouts are only achieved when all alleles of the cell are inactivated, not all cells will have a knockout, leading to a polyclonal situation. In addition, HEK293 cells are pseudo-triploid [Bylund et al., 2004]. Karyotyping of the HEK293 cells showed that chromosome 17, which contains the p53 gene, has three copies [Bylund et al., 2004; McBride et al., 1986]. This extra chromosome makes it more difficult to attain a full knockout. Nevertheless, the HEK293 cell line is still widely utilized as a human cell line in research [Tan, et al., 2021].

In closing, there was no puromycin selection done with the cells used for the western blot and PCR. Because we wanted to save time and we assumed that the vectors containing sgRNAs for p53 and STAT1 were taken up just as well as the pX458-GFP vector. In the future, it could be helpful not to skip the puromycin selection before validation. Furthermore, sgRNA for OAS1 and IFIT1 were incorporated correctly into the backbone vector, therefore further research could proceed with the transfection steps and validation of the resulting KOs could be done. After successfully creating OAS1 and IFIT1 KOs these could be used for research about the inflammatory response induced by CIN, in particular, how this inflammatory response contributes to cell survival in cells with CIN and how aneuploid cancers manage to evade this immune response.

References

Bakhoum, S.F., Ngo, B., Laughney, A.M., Cavallo, J.A., Murphy, C.J., Ly, P., Shah, P., Sriram, R.K., Watkins, T.B.K., Taunk, N.K., Duran, M., Pauli, C., Shaw, C., Chadalavada, K., Rajasekhar, V.K., Genovese, G., Venkatesan, S., Birkbak, N.J., McGranahan, N., Lundquist, M., LaPlant, Q., Healey, J.H., Cleveland, O., Powell, S.N., Lammerding, J., Swanton, C., Cantley, L.C. (**2018**). Chromosomal instability drives metastasis through a cytosolic DNA response. *Nature*, **553**, 467-472.

Ben-David, U., Arad, G., Weissbein, U., Mandefro, B., Maimon, A., Golan-lev, T., Narwani, K., Clark, A.T., Andrews, P.W., Benvenisty, N., Biancotti, J.C. (**2014**). Aneuploidy induces profound changes in gene expression, proliferation and tumorgenicity of human pluripotent stem cells. *Nat. Commun*., **5**, 1.

Bylund, L., Kytola, S., Lui, W.O., Larsson, C., Weber, G. (**2004**). Analysis of the cytogentic stability of the human embryonal kindey cell line 293 by cytogenetic and STR profiling approaches. *Cytogene Genomes Res*. **106**, 28-32.

Cell Signalling Technology. (n.d.) STAT1 Antibody #9172. Retrieved June 7, 2022, from https://www.cellsignal.com/products/primary-antibodies/stat1-antibody/9172

Chen, B., Gilbert, L.A., Cimini, B.A., Schnitzbauer, J., Zhang, W., Li, G., Park, J., Blackburn, E.H., Weissman, J.S., Qi, L.S., Huang, B. (**2013**). Dynamic imaging of genomic loci in living human cells by an optimized CRISPR/Cas system. *Cell*, **155**, 1479-1491.

Chen, M., Linstra, R., & van Vugt, M. (**2022**). Genomic instability, inflammatory signaling and response to cancer immunotherapy. *Biochimica et biophysica acta*. *Reviews on cancer*, **1877**, 188661.

Cheng, A.W., Wang, H., Yang, H., Shi, L., Katz, Y., Theunissen, T.W., Rangarajan, S., Shivalila, C.S., Badon, D.B., Jaenisch, R. (**2013**). Multiplexed activation of endogenous genes by CRISPR-on, an RNA-guided transcriptional activator system. *Cell research*, **23**, 1163-1171.

Di, H., Elbahesh, H., Brinton, M.A. (**2020**). Characteristics of Human OAS1 Isoform Proteins. *Viruses*, **12**, 152.

Duijf, P.H.G., Schultz, N., Benezra, R. (**2013**). Cancer cells preferentially lose small chromosomes. *Int. J. Cancer*, **132**, 2316-2326.

Ebina, H., Misawa, N., Kanemura, Y., Koyanagi, Y. (**2013**). Harnessing the CRISPR/Cas9 system to disrupt latent HIV-1 provirus. *Scientific reports*, **3**, 2510.

Foijer, F., Albacker, L.A., Bakker, B., Spierings, D.C., Yue, Y., Xie, S.Z., Davis, S., Lutum-Jehle, A., Takemoto, D., Hare, B., Furey, B., Bronson, R.T., Lansdorp, P.M., Bradley, A., and Sorger, P.K. (**2017**) Deletion of the MAD2L1 spindle assembly checkpoint gene is tolerated in mouse models of acute T-cell lymphoma and hepatocellular carcinoma. *eLife*, **6**.

Foijer, F., Xie, S.Z., Simon, J.E., Bakker, P.L., Conte, N., Davis, S.H., Kregel, E., Jonkers, J., Bradley, A., and Sorger, P.K. (**2014**). Chromosome instability induced by Mps1 and p53 mutation generates aggressive lymphomas exhibiting aneuploidy-induced stress. *Proc Natl Acad Sci U S A*, **111**, 13427-13432.

Hatch, E.M., Fischer, A.H., Deerinck, T.J., Hetzer, M.W. (**2013**). Catastrophic nuclear envelope collapse in cancer cell micronuclei. *Cell*, **154**, 47-60.

Hellweg, C.E. (**2015**). The nuclear factor κB pathway: a link to the immune system in the radiation response. *Cancer Lett*., **368**, 275-289.

Hong, C., Schubert, M., Tijhuis, A.E., Requesens, M., Roorda, M., van den Brink, A., Andrade Ruiz, L., Bakker, P.L., van der sluis, T., Pieters, W., Chen, M., Wardenaar, R., van der Vegt, B., Spierings, D.C.J., de Bruyn, M., van Vugt, M.A.T.M., Foijer, F. (**2022**). Inhibition of IL6 signalling as a therapeutic strategy to eradicate cancer cells with chromosomal instability. *Unpublished*.

Hou, Y., Liang, H., Rao, E., Zheng, W., Huang, X., Deng, L., Zhang, Y., Yu, X., Xu, M., Mauceri, H., Arina, A., Weichselbaum, R.R., Fu, Y. (**2018**). Non-canonical NF-κB antagonizes STING sensor-mediated DNA sensing in radiotherapy. *Immunity*, **49**, 490-503.

Ishibashi, A., Saga, K., Hisatomi, Y., Li, Y., Kaneda, Y., Nimura, K. (**2020**). A simple method using CRISPR-Cas9 to knock-out genes in murine cancerous cell lines. *Sci Rep*. **10**.

Kadioglu, O., Saeed, M., Mahmoud, N., Azawi, S., Mrasek, K., Liehr, T., Efferth, T. (**2021**). Identification of potential novel drug resistance mechanisms by genomic and transcriptomic profiling of colon cancer cells with p53 deletion. *Archives of Toxicology*, **95**, 959-974.

Mackenzie, K.J., Carroll, P., Martin, C.A., Murina, O., Fluteau, A., Simpson, D., Olova, N., Sutcliffe, H., Rainger, J., Robertson, A., Osborn, R., Wheeler, A., Nowotny, M., Gilbert, N., Chandra, T., Reijns, M.A.M., Jackson, A.P. (**2017**). cGAS surveillance of micronuclei links genome instability to innate immunity. *Nature*, **548**, 461-465.

Mao, Y., Yan, R., Li, A., Zhang, Y., Li, J., Du, H., Chen, B., Wei, W., Zhang, Y., Sumners, C., Zheng, H., Li, H. (**2015**). Lentiviral Vectors Mediate Long-Term and High Efficiency Transgene Expression in HEK 293T cells. International journal of medical sciences, **12**, 407-415.

Marucci, G., Lammi, C., Buccioni, M., Dal Ben, D., Lambertucci, C., Amantini, C., Santoni, G., Kandhavelu, M., Abbrecchio, M.P., Lecca, D., Volpini, R., Cristalli, G. (**2011**). Comparison and optimization of transient transfection methods at human astrocytoma cell line 1321N1. *Analytical biochemistry*, **414**, 300-302.

Musacchio, A. (**2015**). The molecular biology of spindle assembly checkpoint signaling dynamics. *Current Biology*, **25**, 20.

Musacchio, A & Salmon, E.D. (**2007**). The spindle-assembly checkpoint in space and time. *Nat Rev Mol Cell Biol.* **8**, 379-393.

Pidugu, V.K., Pidugu, H.B., Wu, M., Liu, C., Lee, T. (**2019**). Emerging Functions of Human IFIT Proteins in Cancer. *Frontiers in molecular biosciences*, **6**, 148.

Pinto, A.K., Williams, G.D., Szretter, K.J., White, J.P., Proença-Módena, J.L., Liu, G., Olejnik, J., Brien, J.D., Ebihara, H., Mühlberger, E., Amarasinghe, G., Diamond, M.S., Boon, A.C.M. (**2015**). Human and Murine IFIT1 Proteins Do Not Restrict Infection of Negative-Sense RNA Viruses of the Orthomyxoviridae, Bunyaviridae, and Filoviridae Families. *Journal of Virology*, **89**, 18.

Santaguida, S., Richardson, A., Ramalingam Lyer, D., M'Saad, O., Zasadel, L., Knouse, K.A., Wong, Y.L., Rhind, N., Desai, A., Amon, A. (**2017**). Chromosome mis-segregation generates cell cycle-arrested cells with complex karyotypes that are eliminated by the immune system. *Dev. Cell*., **41**, 638-651.

Schubert, M., Hong, C., Jilderda, L.J., Requesens Rueda, M., Tijhuis, A.E., Simon, J.E., Bakker, P.L., Cooper, J.L., Damaskou, A., Wardenaar, R., Bakker, B., Gupta, S., van den Brink, A., Andrade Ruiz, L., Koster, M.H., Youssef, S.A., Luinenburg, D., Strong, A., Engleitner, T., Ponstingl, H., de Haan, G., de Bruin, A., Rad, R., Nijman, H.W., Medema, R.H., van Vugt, M.A.T.M., de Bruyn, M., Spierings, D.C.J., Colomé-Tatché, M., Vassiliou, G.S., Foijer, F. (**2021**). Cancer tolerance to chromosomal instability is driven by STAT1 inactivation in vivo. *bioRxiv* 471107.

Schukken, K.M. & Foijer, F. (**2017**). CIN and Aneuploidy: Different Concepts, Different Consequences. *BioEssays*, **40**, 1.

Shaw, G., Morse, S., Ararat, M., Graham, F.L. (**2002**). Preferential transformation of human neuronal cells by human adenoviruses and the origin of HEK 293 cells. *The FASEB Journal*. **16**, 869-871

Shojaei Baghini, S., Gardanova, Z.R., Zekiy, A.O., Shomali, N., Tosan, F., Jarahian, M. (**2021**). Optimizing sgRNA to improve CRISPR/Cas9 knockout efficiency: special focus on human and animal cell. Front Bioeng Biotechnol. **9**.

Simonetti, G., Bruno, S., Padella, A., Tenti, E., Martinelli, G. (**2019**). Aneuploidy: Cancer strength or vulnerability? *Int J Cancer*, **144**, 8-25.

Sun, L., Lutz, B.M., Tao, Y. (**2016**). The CRISPR/Cas9 system for gene editing and its potential application in pain research. *Transl Perioper Pain Med*. **1**, 22-33.

Sun, L., Shen, X., Liu, Y., Zhang, G., Wei, J., Zhang, H., Zhang., E., Ma, F. (**2010**). The location of endogenous wild-type p53 protein in 293T and HEK293 cells expressing low-risk HPV-6E6 fusion protein with GFP. *Acta biochimica et biophysica Sinica*, **42**, 230-235.

Synthego. (n.d.). HEK293 Cells: Background, Applications, Protocols, and More - A Guide to One of the Most Commonly Used Cell Lines. Synthego. Retrieved may 29, 2022, from https://www.synthego.com/hek293

Tan, E., Chin, C.S.H., Lim, Z.F.S, Kong Ng, S. (**2021**). HEK293 Cell Line as a Platform to Produce Recombinant Proteins and Viral Vectors. *Front. Bioeng. Biotechnol.*, **13**.

Thomas, P. & Smart, T.G. (**2005**). HEK293 cell line: A vehicle for the expression of recombinant proteins. *Journal of Pharmacological and Toxicological Methods*, **51**, 187-200.

Tuladhar, R., Yeu, Y., Piazza, J.T., Tan, Z., Clemenceau, J.R., Wu, X., Barret, Q., Herbert, J., Mathews, D.H., Kim, J., Hwang, T.H., Lum, L. (**2019**). CRISPR-Cas9-based mutagenesis frequently provokes on-target mRNA misregulation. *Nature Communications*, **10**, 4056.

Vannucci, L., Lai, M., Chiupessi, Fl., Ceccherini-Nelli, L., Pistello, M. (**2013**). Viral vectors: a look back and ahead on gene transfer technology. *New Microbiologica*, **36**, 1-22.

Wan, L., Wang, Z., Tang, M., Hong, D., Sun, Y., Ren, J., Zhang, N., Zeng, H. (**2021**). CRISPR-Cas9 gene editing for fruit and vegetable crops: strategies and prospects. *Horticulturae*, **7**, 193.